

DETERMINATION OF THE BEAM WIDTH IN A STELLATRON ACCELERATOR

H. Ishizuka, R. Prohaska, A. Fisher and N. Rostoker
Physics Department
University of California
Irvine, CA 92717

Abstract

The UCI stellatron is a strong focusing, high current betatron that accelerates a 1 kA electron beam. To measure the minor dimension of the beam, targets were inserted at different radii from the outer side of the torus. The beam was swept outward by applying a pulsed vertical magnetic field. Time dependence of the X-ray emission from the target was analyzed to determine the expansion velocity and the density distribution of the beam. 50% and 90% of the electrons were found within 4 mm and 7 mm radii, respectively, at 5 MeV.

Introduction

The UCI stellatron project has been concerned with problems relative to generating a 1 kA 10 MeV beam [1,2]. That goal has been reached [3], although decay of the beam current during acceleration has not been fully obviated yet. We are now concerned about the quality of the beam.

In the past, a two probe method that analyzed X-rays from inner and outer targets was successfully used to determine the distribution of electrons in both betatron amplitude and momentum [4,5]. We have employed a similar method, but the inner target was not allowed with our device. Since the betatron oscillation in a stellatron appears as gyration about the minor axis, the introduction of an X-ray target at a particular distance from the beam axis selectively scrapes off electrons with an oscillation amplitude greater than the distance from the beam center to the target. By shifting the beam center toward the target, therefore, we progressively sample the population distribution of electrons.

Apparatus

The experimental arrangement is schematically shown in Fig. 1. Details were described elsewhere [3]. Targets were placed at east, west and southeast ports. They were thin tungsten wires initially to minimize

the effect on the beam. It turned out that the X-rays from the torus wall had influence on the measurement along with a noise. After examination for different thicknesses, most of the data in this paper were taken with brass targets which were 4 cm high and 6 mm wide. The thickness in the azimuthal direction was 1/8", which was close to the range of 5 MeV electrons. Lead targets were used when large X-ray signals were required to improve the S/N ratio (e.g. Fig. 4b). Spiller loops for expanding the beam orbit [2] were attached on the inner and outer sides of the torus. Now that they were wound over the helical windings, the distance from the minor axis of the torus to the loops was approximately 5.6 cm. The outer windings were not axisymmetric, since they were steered clear of the ports. A current was fed from a 0.05 μ F capacitor charged up to 60 kV.

Experiment

The west target served as a limiter and also as a source of X-rays for monitoring the beam. It was so placed that the front was at 18 mm from the outer wall of the torus. This position was chosen for two reasons; First, the beam current decreased if the target was moved further inward. Second, the expansion speed of the orbit increased near the torus wall. For analysis of the experimental data it was desirable that the speed was nearly constant in the relevant region. The east target was fixed at 5 mm inside from the torus wall. The southeast target was moved radially, as mentioned later. PIN diodes were aimed at each of the targets. The betatron condition was adjusted so as to maximize the beam current in the presence of the targets. The beam did not disrupt abruptly [3] as long as it was scraped by one of the targets. The machine was operated at an interval of 10 minutes and consistently generated a 0.9 - 1.1 kA 5 MeV beam. The peak toroidal magnetic field was 15 kG, and the helical field gave a rotational transform angle $1/2\pi$ of approximately 0.1.

X-rays were not detected at the east target throughout this experiment, indicating that all the beam electrons hit the target located radially inward. The southeast target did not yield X-rays if it was placed near the torus wall. When the spiller field was not applied, X-rays began to appear at the southeast target as its radial position was changed close to that of the west target. Further shift of the southeast target by 2 mm caused disappearance of X-rays at

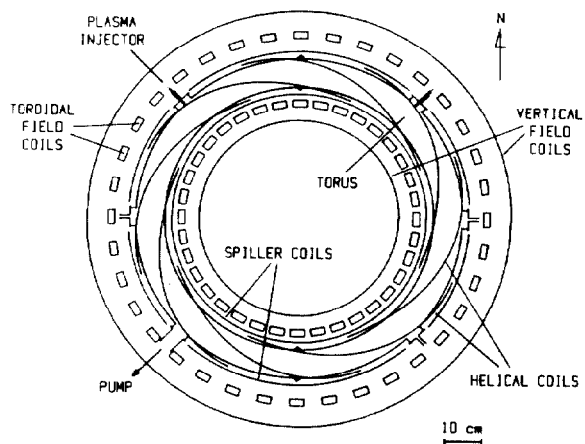


Fig. 1. Top view of the UCI stellatron.

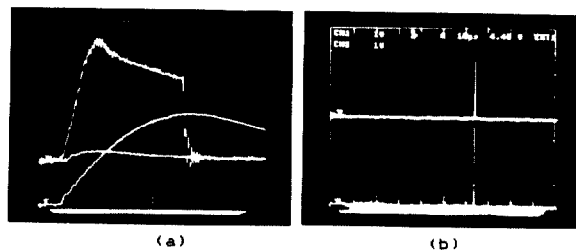


Fig. 2. (a) Upper trace: beam current, 322 A/div. Lower trace: betatron flux. (b) X-rays from the west and southeast targets. Sweep: 10 μ s/div.

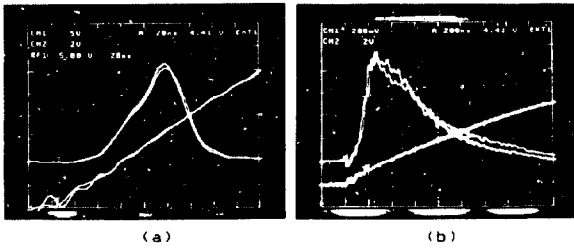


Fig. 3. X-ray signals for (a) fast and (b) slow orbit expansion. Lower traces are spiller current, 362 A/div. Sweep: (a) 20 ns/div and (b) 200 ns/div.

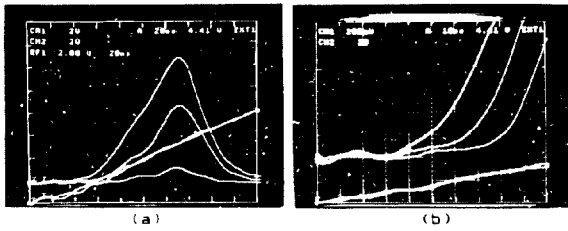


Fig. 4. X-rays for different target positions. (a) The largest signal is for the normal position, middle and the smallest are for 0.5 mm and 2 mm outside, respectively. 20 ns/div. (b) Early stage. The target position was changed by a 1 mm step. 10 ns/div.

the west target. The normal position of the southeast target was so chosen that the X-rays from the two targets were equal.

The spiller was activated near the peak of the betatron field and terminated the beam current as shown in Fig. 2a. PIN diodes aimed at the west and southeast targets detected a burst of X-rays at that moment (Fig. 2b). X-rays continuously generated during acceleration are not seen here because their intensity was smaller than the burst by two orders of magnitude. The spiller current I_{sp} increased linearly with time. Figure 3a shows an X-ray burst for $dI_{sp}/dt = 12 \text{ kA}/\mu\text{s}$. The signal was characterized by a faster decay relative to the rise when $dI_{sp}/dt > 6 \text{ kA}/\mu\text{s}$. The waveform of the X-ray burst changed if the rise rate of the spiller current was reduced, as shown in Fig. 3b for $dI_{sp}/dt = 0.9 \text{ kA}/\mu\text{s}$; the peak of the signal shifted to the earlier phase.

When the target was moved outward, the signal became smaller and its start was delayed. Figure 4a shows the X-ray burst from the southeast target set at the normal position, 0.5 mm outside and 2 mm outside. The expansion speed of the beam orbit was determined from the delay of the signal. For this purpose, the PIN diode was moved closer to the port as the target was shifted outward, so that the size of the X-ray signal was nearly the same (Fig. 4b). The expansion speed was 0.11 mm/ns for $dI_{sp}/dt = 10 \text{ kA}/\mu\text{s}$ and changed in proportion to dI_{sp}/dt .

X-ray pinhole pictures were taken of the targets with a camera having a 1 mm aperture. Films were sensitive to X-rays that passed through the body of the camera (1" thick lead), and so the image of the

target was not very clear. The picture of the innermost target was exposed by X-rays generated during acceleration and not used to see the structure of the beam. The southeast target gave a measure, when it was shifted outward by 1 - 2 mm from the normal position, that X-rays were produced over a vertical range with an 8 - 10 mm width.

Beam Width

The density profile of a circulating beam is determined by the spread in betatron amplitude and the spread in momentum. Without an inner target, the density profile can be analyzed when either one of those dominates. Our experiment showed that the X-ray signal changed its shape with dI_{sp}/dt . This suggests that the spread in the betatron amplitude is dominant, because the betatron oscillation can grow during expansion due to the asymmetry of the spiller field but the momentum distribution should not change significantly. (The mutual inductance between the spiller loops and the beam is less than 0.4 μH , and the energy change caused by the spiller field is smaller than 1%.) That the accelerated beam does not have a large momentum spread and also that the momentum compaction factor is small for a stelleron support this view. Based on these considerations, we assume that the betatron oscillation is responsible for the beam width.

The betatron motion in a stelleron is regarded as circular around the minor axis of the beam [6]. Then the electron density $n(r)$ is simply given by $N(r)/2\pi r$, where r is the distance from the minor axis and $N(A_b)$ is the distribution in the betatron amplitude A_b . Let us denote radial positions of the target and the beam center as R_t and R_c , respectively. When the beam orbit expands, electrons having A_b larger than $R_t - R_c$ get a chance to hit the target. The probability for the electron to be at a radial position $R > R_t$ is given by $P(R > R_t) = \cos^{-1}((R_t - R_c)/A_b)/\pi$. In one gyration period t_g around the torus, $P(R > R_t) \times N(A_b)$ is taken by the target. If the expansion velocity is v and electrons are intercepted by two targets as in our case, $N(A_b)$ changes with time as

$$\frac{dN(A_b)}{dt} = -\frac{N(A_b)}{\pi t_g} \left[u(t-t_1) \cdot \cos^{-1}\left(1-v \frac{t-t_1}{A_b}\right) + u(t-t_2) \cdot \cos^{-1}\left(1-v \frac{t-t_2}{A_b}\right) \right], \quad (1)$$

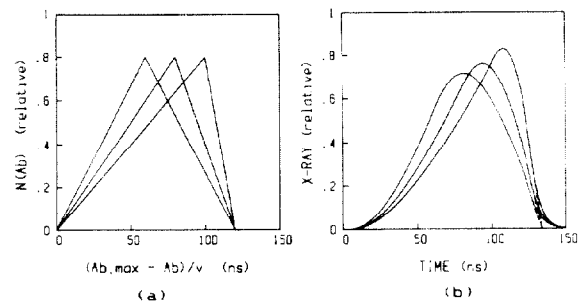


Fig. 5. Electron distribution in betatron amplitude. (b) X-ray waveforms calculated for $N(A_b)$ given in (a).

where $t_1 = (A_{b,max} - A_b)/v$ and $t_2 = (A_{b,max} + d - A_b)/v$, d being the radial position of the second target measured from the normal position. $u(x)$ is the unit step function and time t is measured from the instant when the outer edge of the beam contacts the first target. The first and second terms on the right hand side of Eq. (1) are proportional to the X-ray intensities from the first and second targets, respectively. Equation (1) is solved analytically, and the X-ray signals from the two targets are calculated if initial $N(A_b)$ is given.

Let us consider the distribution $N(A_b)$ as shown in Fig. 5a. Here $A_{b,max}/v$ is 120 ns, at which time the beam center ($A_b = 0$) reaches the target. Waveforms of the X-ray intensity calculated for $d = 0$ are independent of v and shown in Fig. 5b. In comparison with $N(A_b)$, the X-ray waveform rises more slowly, has a rounded top, and is delayed as a whole. Note that the curves in Fig. 5b bear resemblance to X-ray signals observed (Figs. 3a and 4a).

The actual problem is how to find $N(A_b)$ that gives an X-ray waveform that matches the experimental signal. Repeated computation of the X-ray waveform changing $N(A_b)$, until a sufficient agreement is found with the signal, leads to the solution. Another way is to use the relation between $N(A_b)$ and the X-ray waveform as illustrated in Fig. 5. The experimental X-ray signal is simulated by superposing the curves in Fig. 5b with certain weights. $N(A_b)$ is obtained as a weighted mean of the original distributions. Accuracy is improved by increasing the number of the curves used. The third way, which is the simplest, is as

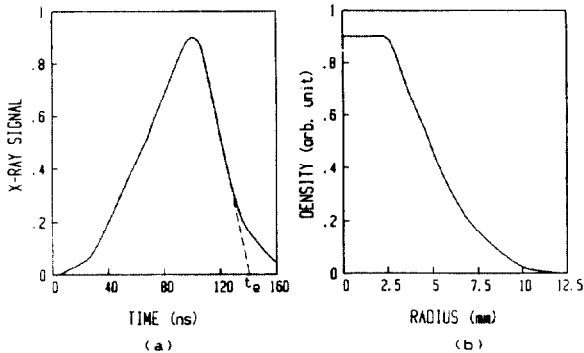


Fig. 6. (a) X-ray signal for an expansion velocity of 0.082 mm/ns. (b) Electron density profile.

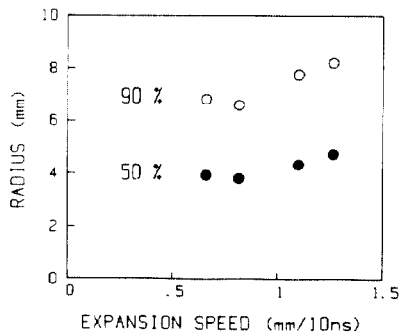


Fig. 7. Beam radii containing 50 % and 90 % electrons.

follows: We modify the downward curves in Fig. 5b as shown by the dotted lines and assume that the X-ray waveform represents $N(A_b)$.

These three methods were applied to a typical X-ray signal, and beam radii containing 50% and 90% of electrons were derived. The results agreed with each other within 10%, and thereafter the third method was mainly adopted to analyze the data. An X-ray signal from the southeast target set at the normal position ($d=0$) is given in Fig. 6a. The electron density distribution (Fig. 6b) is obtained by a relation $n(r) \propto X(t)/v(t_e - t)$, where $X(t)$ is the X-ray intensity at time t and t_e is the end point of the dotted line. The radii that contain 50% and 90% of electrons are shown in Fig. 7. For expansion velocities of 0.7 - 0.9 mm/turn, they are 4 mm and about 7 mm, respectively.

The above treatment was extended to evaluate the vertical distribution of X-ray intensity on the target. Inconsistency was not found with X-ray pinhole picture data.

Discussion

We have assumed smooth expansion of the orbit. Small discrepancies were found between experiment and calculation; e.g. the observed tail of the X-ray signal was larger than calculated (Figs. 5b and 6a). This is qualitatively explained as follows: The beam center oscillates around an expanding circle due to the toroidal magnetic field, and the oscillation introduces an apparent increase in the beam width. As the amplitude increases with expansion velocity, larger radii observed for faster expansion (Fig. 7) may be attributed to this effect. Taking into account also the possible growth of the betatron amplitude during expansion, we may assume that the experiment gave the upper limit on the width of the beam. The current density observed in this work exceeded 1 kA/cm^2 around the minor axis.

Acknowledgement

This work was supported by the Office of Naval Research.

References

- [1] B. Mandelbaum, H. Ishizuka, A. Fisher and N. Rostoker, *Phys. Fluids* **31**, 916 (1988).
- [2] H. Ishizuka, A. Fisher, K. Kamada, R. Prohaska and N. Rostoker, 87CH2387-9 (Proc. 1987 IEEE Particle Accelerator Conference), p. 136.
- [3] H. Ishizuka, R. Prohaska, A. Fisher and N. Rostoker, *Proc. Int. Conf. on High Power Particle Beams*, 1988, p. 857.
- [4] J. M. Peterson and J. B. Rechen, *IEEE Trans NS-20*, 790 (1973).
- [5] G. R. Lambertson, W. W. Chupp, A. Faltens, E. C. Hartwig, W. J. Herrmann, D. Keefe, L. Jackson Laslett, J. M. Peterson, J. B. Rechen and A. Salop, *Part. Accel.* **5**, 113 (1973).
- [6] C. W. Roberson, A. Mondelli and D. Chernin, *Part. Accel.* **17**, 79 (1985).